QRS duration reflects underlying changes in conduction velocity during increased intraventricular pressure and heart failure.

Authors: Jorge G. Quintanilla,[1,2,3] Javier Moreno,[3, 4] Tamara Archondo,[2,5] José Manuel Alfonso-Almazán,[1] José María Lillo-Castellano,[1,6] Elena Usandizaga,[2,3] María Jesús García-Torrent,[2,3] Cruz Rodríguez-Bobada,[2] Pablo González,[2] Luis Borrego,[2] Victoria Cañadas-Godoy,[2,3], Juan J. González-Ferrer,[2,3] Nicasio Pérez-Castellano,[2,3] Julián Pérez-Villacastín,[2,3] David Filgueiras-Rama.[1,2,3]

[1] Fundación Centro Nacional de Investigaciones Cardiovasculares, Carlos III (CNIC), Myocardial Pathophysiology Area. Madrid, Spain.

[2] Instituto de Investigación Sanitaria del Hospital Clínico San Carlos (IdISSC). Department of Cardiology. Madrid, Spain.

[3] CIBER de Enfermedades Cardiovasculares.

[4] Hospital Universitario Ramón y Cajal. Department of Cardiology. Madrid, Spain.

[5] Hospital General Universitario Santa Lucía. Department of Cardiology. Cartagena, Murcia, Spain.

[6] Universidad Rey Juan Carlos. Department of Signal Theory and Communications, Telematics and Computing. Madrid, Spain.

Corresponding author:

David Filgueiras-Rama, MD, PhD
Fundación Centro Nacional de Investigaciones Cardiovasculares, Carlos III/ Spanish National Cardiovascular Research Center (CNIC)
Myocardial Pathophysiology Area
Melchor Fernández Almagro, 3, 28029, Madrid, Spain
Email: david.filgueiras@cnic.es
Tel. +34-914531200. Ext 1510/4305/1508

ABSTRACT

Pressure overload and heart failure electrophysiological remodeling (HF-ER) in pigs are associated with decreased conduction velocity (CV) and dispersion of repolarization, which lead to higher risk of ventricular arrhythmia. This work aimed to establish the correlation between QRS complex duration and underlying changes in CV during increased intraventricular pressure (IVP) and/or HF-ER *ex-vivo*, and to determine whether QRS duration could be sensitive to an acute increase in left ventricular afterload *in-vivo*. HF-ER was induced in 7 pigs by high-rate ventricular pacing. Seven weight-matched controls were used as controls. Isolated Langendorff-perfused hearts underwent programmed ventricular stimulation to study QRS complex duration and CV under low/high IVP, using volume-conducted ECG and epicardial optical mapping, respectively. Four additional pigs underwent open-chest surgery to increase left ventricular afterload by partially clamping the ascending aorta, while measuring QRS complex duration during SR. In 13 hearts included for analysis, both HF-ER and increased IVP showed significantly slower epicardial CV (-40% and -15%, $p<0.001$ and $p=0.004$, respectively), which correlated with similar widening of the QRS complex (+41% and +17%, $p=0.005$ and $p<0.001$, respectively). HF-ER hearts shower larger prolongation of the QRS complex than controls upon increasing the IVP (+21% vs. +12%, respectively. HF-ER*IVP interaction: $p=0.004$). QRS complex widened after increasing LV afterload *in-vivo (n=3),* with correlation between QRS duration and aortic diastolic pressures ($R=0.58$,$p<0.001$). In conclusion, high IVP and/or HF-ER significantly decrease CV, which correlates with QRS widening on the surface ECG during ventricular pacing. Increased myocardial wall stress also widens the QRS complex during SR *in-vivo*.

Keywords: Heart failure; intraventricular pressure; remodelling; afterload; optical mapping.

1. Introduction

A common hemodynamic change as heart failure (HF) evolves and left ventricular dysfunction gradually decreases, is the presence of increased intraventricular pressures (IVPs),(Zile et al., 2011) which indeed may vary in time depending on heart functional status and treatment.(Abraham and Hayes, 2003) A clinical estimate of left ventricular diastolic pressure and pulmonary capillary wedge pressures, can be obtained from estimated pulmonary artery diastolic pressure (ePAD) or actual pulmonary artery pressures using implantable hemodynamic monitors.(Magalski et al., 2002; Ohlsson et al., 1995); (Costanzo et al., 2016) Hemodynamic changes monitored with such devices have been associated with clinical outcomes such as acute decompensated HF,(Zile et al., 2008) heart failure-related hospitalizations,(Bourge et al., 2008) and mortality.(Abraham et al., 2011; Zile et al., 2017) Moreover, subject-normalized elevation in ePAD has been associated with the occurrence of ventricular arrhythmic events compared with periods of euvolemia and subject-specific baseline pressure.(Reiter et al., 2013)

Experimental data from a pig model of HF also support that increased IVPs are as harmful as heart failure electrophysiological remodeling (HF-ER) on favoring ventricular arrhythmia.(Quintanilla et al., 2015) Thus, increased IVPs were associated with a decrease in conduction velocity (CV) by ≈20% and an increase in dispersion or repolarization by ≈30%, obtained from voltage–sensitive optical recordings. Such electrophysiological changes increased the risk of ventricular arrhythmia upon programmed ventricular stimulation compared with controls. Theoretically, a decrease in CV from optical mapping recordings in isolated hearts should correlate with widely available clinical parameters as QRS widening on the surface ECG of HF patients with deteriorated hemodynamic status. The clinical value of such a non-invasive parameter become especially relevant since nowadays continuous monitoring of ventricular pressures in patients with HF requires invasive strategies by means of additional sensor leads, which limits its clinical implementation. In fact, these additional leads are not exempt of complications and lead failure.(Adamson et al., 2011)

Therefore, a non-invasive parameter as QRS duration, which can be easily obtained from implantable cardioverter defibrillators (ICD) or cardiac resynchronization therapy devices (CTR) using current remote monitoring technology and can-tip/coil lead configurations, may have the potential to be useful in assessing the risk of HF events in patients with chronic HF. This work aims to establish the correlation between QRS complex duration and underlying changes in CV during increased IVP and/or HF-ER in optically mapped Langendorff-perfused pig hearts. We also aim to determine whether QRS complex duration can also be sensitive to an acute increase in left ventricular afterload during sinus rhythm *in-vivo*. We hypothesize that HF-ER and/or increased IVP in Langendorff-perfused isolated hearts will decrease CV, which will lead to widening of the QRS complex on the ECG. We also hypothesize that QRS duration on the surface ECG will reflect the effects of an acute increase in left ventricular afterload,

2. Material and methods

The study was divided into two experimental settings to achieve the study aims: *i)* Isolated Langendorff-perfused hearts undergoing voltage optical mapping and QRS

complex duration measurements from volume-conducted ECG recordings, and *ii)* pigs undergoing increased left ventricular afterload *in-vivo,* while QRS complex duration is continuously monitored from the surface ECG.

All surgical procedures were performed under deep anesthesia (ketamine 20 mg/kg, propofol 6 mg/kg, atracurium besylate 0.2 mg/kg and 1.25 mg/ (kg h), fentanyl 0.005 mg/(kg h), and isoflurane 2%). The experimental studies were conducted in accordance with institutional guidelines and National (ECC/566/2015, RD53/2013) and European (2010/63/EU) regulation guidelines for the care and use of laboratory animals. All *in-vivo* experimental procedures were evaluated and granted by the Institutional Animal Care and Use Committee (IACUC) of Hospital Clínico San Carlos and the Local Competent Authority.

2.1 Heart failure model and experimental protocol in the Langendorff-Perfused pig heart

HF was induced in 7 Pietrain pigs by high-rate ventricular pacing (190 beats/min) for ~4 weeks until clear symptoms of HF developed as reported elsewhere.(Quintanilla et al., 2015) Seven pigs did not undergo pacemaker implantation and were used as controls. Excised hearts from ~40 Kg pigs were connected to a Langendorff perfusion apparatus as described elsewhere.(Quintanilla et al., 2015) Hearts were perfused and superfused with warm Tyrode's solution (37ºC). Upon the heart reached a temperature of 37ºC, it was defibrillated to sinus rhythm. Ten ECG electrodes were randomly but homogeneously distributed within the superfusion Tyrode's solution to generate a volume-conducted ECG (Figure 1A). Briefly, optical recordings and volume-conducted ECG were obtained under low or high IVP, both in hearts with HF and controls. The electromechanical uncoupler blebbistatin was not used as it has been reported to have significant electrophysiological effects.(Brack et al., 2013) We relied on a mechanical approach to reduce motion by gently compressing the heart against the inner surface of the imaging window of the superfusion chamber, only for the time needed to record the set of movies at each experimental setting.

Increased IVP was achieved by inflating a fluid-filled balloon to increase the LV end-diastolic pressure from ~0 mm Hg (low IVP) to ~20 mm Hg (high IVP). An electrophysiological recording system (Prucka CardioLab, General Electric Medical, Milwaukee, USA) was used to continuously monitoring volume-conducted ECG (sample rate: 1KHz), perfusion pressure, and IVP, while keeping the perfusion pressure always higher than the IVP in order to prevent subendocardial ischemia.

Optical mapping data were obtained from the anterior surface of the left ventricle. The programmed stimulation protocol consisted of a ventricular pacing train (S1, 8 pacing beats) at 500 and 300 ms basic drive cycle length (BDCL) + 1 pacing beat (S2), 10 ms over the effective refractory period, from the left upper corner of the field of view. We recorded the local emitted fluorescence (Di-4-ANEPPS, 800 frames per second) from S1 and S2 epicardial wavefronts. Optical data from isolated heart preparations were partially reported in our previous publication.(Quintanilla et al., 2015) In one HF-ER heart, optical mapping was not performed due to unsolvable technical problems at the time of the experiment.

2.2. Data processing and analysis from Langendorff-Perfused hearts

Prior to any analysis and regardless of the filed of view, movies were masked to always analyze a 3x3 cm2 area to ensure that measurements were comparable among hearts and to diminish the effects of 3D propagation. Then, the activation dynamics of S1 and S2 waves were analyzed using custom-made software as reported elsewhere. (Quintanilla et al., 2015) Briefly, the optical measurements at each setting (HF - yes/no - or IVP –high/low-) were routinely averaged from movies under identical conditions. Activation time of each pixel was calculated at the time of (dV/dt)max after suitable preconditioning (cone-shaped kernel time-space smoothing) and filtering (zero-phased 50th-order low-pass Butterworth filter). Local velocity vectors, representing the magnitude and direction of conduction velocity at each recording site, were computed as previously described (Quintanilla et al., 2015). Briefly, to avoid overestimation of velocities due to similar activation times in adjacent pixels, the matrix containing activation times was down-sampled by 4. Then, the resulting activation times were fitted with a cubic smoothing spline surface resulting in a scalar field that described local activation times as a function of position (Figure 1B). Assuming that propagation is normal to the wavefront at each point, through the gradient of this function we can obtain a vector field with the local CV at each location. Before averaging, the residual spurious values of CV caused by simultaneous capture of tissue, adjacent to the pacing site (virtual electrode), were discarded and excluded from analysis. Then, we measured the averaged CV magnitude (CVmean) in the whole field of view that includes mainly, but not exclusively, the longitudinal component of CV".

Twelve ECG leads were obtained from 10 ECG electrodes submerged in the superfusion Tyrode´s solution. QRS duration was manually measured at 200 mm/sec sweep-speed, from the lead with the earliest deflection (positive or negative) to the lead with the latest offset of the QRS complex. Two hearts with HF were excluded from volume-conducted ECG analysis due to poor signal-to-noise ratio.

2.3. Experimental protocol in pigs undergoing increased left ventricular afterload in-vivo

Four additional pigs (~40 Kg) without HF were used for *in-vivo* evaluation of QRS widening upon increasing left ventricular afterload, while conduction is preserved through the His-Purkinje system. After general anesthesia pigs underwent cannulation of the left and right femoral artery to position two 8F introducers and further progress a pigtail catheter to the ascending aorta (proximal), next to the aortic valve, and a second pigtail catheter to the thoracic descending aorta (distal). Proper positioning of both pigtail catheters was confirmed by fluoroscopy (Figure 2A,B). Then, animals underwent open-chest surgery to expose the ascending aorta and the anterior part of heart (Figure 2A). Carefully separation of the ascending aorta and the main pulmonary artery was performed to enable introducing a surgical clamp that embraces the aorta above the proximal pigtail catheter (Figure 2B). After baseline recordings of surface ECG (6 limb leads, V1 and V6) and aortic pressures, left ventricular afterload was progressively increased upon partial closure of the aortic clamp. ECG recordings, proximal and distal aortic pressures were digitally monitored and acquired at 100 samples/second (anesthetic equipment Carecape Monitor, Datex-Ohmeda, General Electric Medical, Milwaukee, USA). Then, the acquired signals were exported to 'comma separated values' files using proprietary software (S/5 software, Datex-Ohmeda, General Electric Medical,

Milwaukee, USA) and imported into Matlab. Customized Matlab software was used to measure QRS width and aortic pressure values and trends (Figure 2C). ECG signals were interpolated (10x) between samples, which resulted in a post-interpolation sampling rate of 1000 samples/s. This interpolation was needed to increase accuracy on detecting the QRS onset and offset. Systolic and diastolic aortic pressures from proximal and distal aortic recordings were compared on beat-to-beat bases with QRS complex duration. Surface-ECG signals from one pig did not enable to obtain reliable measurements of the QRS duration due to continuous noise artifacts. Therefore the results were obtained from 3 pigs.

2.4. Statistical Analysis

The Shapiro-Wilk test was used to test continuous variables for normality. The independence assumption prohibits application of generalized linear models to correlated data. Nevertheless, Generalized Estimating Equations (GEE) were developed to extend generalized linear models to accommodate correlated data. The only model assumptions are that individual measurements are assumed to be dependent within subjects and independent between subjects. The correlation matrix that represents the within-subject dependencies is estimated as part of the model. Thus, a mixed model with GEE was used to test for significant differences and interactions in *ex-vivo* CV and QRS data, using subject identifier as the *'subject'* factor, remodeling (control or HF-ER) as a *'between-subjects'* factor and 3 *'within-subjects'* factors (repeated measures): IVP (low or high), BDCL (500 or 300 ms) and type of beat (S1 or S2). Pearson's coefficient was used to assess the degree of correlation between *in-vivo* QRS measurements and proximal aortic systolic/diastolic pressures. Continuous variables are expressed as mean±SEM. A two-tailed $p<0.05$ was considered statistically significant.

3. Results

3.1. Heart failure-electrophysiological remodeling and increased intraventricular pressure decrease conduction velocity in isolated-heart preparations

Epicardial CV was significantly slower in HF-ER hearts (average -40%; $p<0.001$). CV also significantly decreased after increasing IVP (average -15%; $p=0.04$. Figure 3A). Pacing at 300 ms BDCL and upon introducing S2 extrastimuli slowed propagation by 17% ($p<0.001$) and 20% ($p<0.001$), respectively. Results from tests of model effects and relative change in paired measurements of CV are shown in Figure 3B,C.

The following significant interactions were found: HF-ER hearts were more prone to decrease CV when pacing at 300 ms BDCL (300 ms BDCL: -49% vs. 500 ms BDCL: -32%, HF-ER*BDCL interaction: $p=0.019$) and during S1 pacing (S1: -43% vs. S2: -37%, HF-ER*Extra interaction: $p=0.011$). Moreover, the decrease in CV at S2 stimuli was more pronounced when pacing at 500 ms BDCL (500 ms BDCL: -23% vs. 300 ms BDCL: -15%, BDCL*Extra interaction: $p=0.004$).

3.2. Heart failure-electrophysiological remodeling and increased intraventricular pressure prolonged QRS duration in isolated-heart preparations

QRS duration was longer in HF-ER hearts than in controls (average increase: +41%, p=0.005). A significant prolongation of QRS duration was also observed upon increasing IVP (average prolongation considering all hearts and conditions: +17%, p<0.001) (Figure 4A). Of note, this prolongation was more pronounced in HF-ER hearts than in controls as shown by a significant HF-ER*IVP interaction (prolongation in controls: +12% vs. HF: +21%, p=0.004) (Figure 4B). Pacing at 300 ms BDCL and after including S2 extraestimuli, QRS duration increased on average by +14% (p=0.001) and +25% (p<0.001), respectively (Figure 4B,C). Results from tests of model effects and relative change in paired measurements of CV are shown in Figure 4A,C. Actual values of QRS duration and 2-way interactions are shown in Table 1. Figure 5 shows two examples of QRS prolongation upon high IVP in both a control heart (top panel) and a failing heart (bottom panel).

3.3. Increased left ventricular afterload during sinus rhythm prolongs QRS duration in-vivo

A total of 1186 sinus rhythm QRS complexes from 3 pigs and their simultaneous aortic pressures were analyzed. Partial clamping of the ascending aorta progressively increased both systolic and diastolic pressures in the ascending aorta (aortic root) and decreased them in the descending aorta. Within 297±183 seconds the aortic root pressures were progressively increased up to 270 mmHg (systolic) and 165 mmHg (diastolic). Figures 6A,B display scatterplots showing a high negative correlation between both systolic and diastolic pressures at the aortic root and descending aorta upon partial clamping. Interestingly, Pearson's coefficient analysis showed statistically significant correlation between QRS duration and proximal aortic pressures (p<0.001), with slightly higher correlation (R=0.58) between QRS duration and diastolic aortic values than systolic values (R=0.54) (Figure 6C,D, respectively). Figure 7 shows an example of QRS lengthening upon increasing left ventricular afterload.

4. Discussion

This study shows that either HF-ER or high IVP in normal hearts, were associated with a significant decrease in CV on the epicardial surface of the left ventricle. The latter correlated with widening of the QRS complex from volume-conducted ECG tracings upon programed ventricular stimulation. Complementary experiments *in-vivo* also showed that an increase in left ventricular afterload, which indirectly increases left ventricular end diastolic volume and pressure,(Fukuta and Little, 2008) significantly widens the QRS duration during sinus rhythm.

Myocardial wall stretch has been previously associated with slower CV compared to baseline conditions without stretch.(Eijsbouts et al., 2004) In fact, a more depolarized resting membrane potential under stretch may partially explain such a slower CV.(Kamkin et al., 2003) Therefore, in control hearts stretch-related decrease of CV seems the main mechanism explaining QRS complex widening on the surface ECG. In failing hearts, CV is already slower than in controls at low IVP, which may be explained by HF-related ionic remodeling (e.g. decrease in Na^+ current),(Nattel et al., 2007) myocardial dilation and the presence of myocardial heterogeneities (e.g. fibrosis) that will increase wave propagation times. Interestingly, upon increasing stretch CV further decreases and QRS complex

widens, which reflects that stretch-related decrease of CV is also one of the mechanisms underlying QRS widening in failing hearts.

The relevance of monitoring hemodynamic changes to optimize treatment in patients with HF has demonstrated to significantly decrease HF-related hospitalizations and increase freedom from first HF-related hospitalization or mortality.(Abraham et al., 2011) These outcomes were related to more frequent adjustment of pharmacologic interventions, mainly diuretic and vasodilator medications, compared with changes triggered by clinical signs and symptoms alone.(Costanzo et al., 2016) Unlike the effect of pressure sensor-based pharmacologic interventions on clinical outcomes, there is no demonstration to date that pharmacologic adjustment may also decrease arrhythmic events. The latter will require much larger series since arrhythmic events as ventricular fibrillation or polymorphic ventricular tachycardia are far less common (4.5% after a mean follow up >2.5 years) than HF-related hospitalizations (>20% after 6 months of follow up).(Abraham et al., 2011; Lillo-Castellano et al., 2016) New remote monitoring capabilities from current ICD or CRT-D devices certainly open the possibility to include large number of patients and achieve statistical significance for decreasing arrhythmic events using pressure sensor-based pharmacologic adjustment in patients with HF. It is also relevant that hemodynamic changes associated with decompensated HF are generally detectable about 2 to 4 weeks before a hospitalization using implantable sensors and data revision at least once a week.(Abraham et al., 2011; Stevenson et al., 2010) The latter would be also feasible, or even improved, by monitoring QRS complex duration obtained during ventricular pacing from automatic or manual remote transmissions using a can-tip/coil configuration, specially considering that HF hearts are more sensitive to widen the QRS complex than controls upon increasing IVP.

From the foregoing, it seems clear that accurately monitoring QRS complex lengthening may have significant clinical impact if changes are associated with acute or sub-acute hemodynamic deterioration in HF. Despite these changes may be large enough to be detected using appropriate automated algorithms during single chamber ventricular pacing (similar to our stimulation protocol in Langendorff-perfused hearts), such differences may be less pronounced during bi-ventricular pacing or sinus rhythm. Our data suggest that acute hemodynamic changes may also be reflected in QRS complex duration during sinus rhythm. Thus, increased left ventricular afterload led to significant lengthening of the QRS complex despite the Purkinje system could theoretically (if it does not participate in conduction slowing) minimize any underlying delayed propagation. Unlike human Purkinje fiber distribution, which is limited primarily to the endocardial surface,(Forsgren et al., 1982) Purkinje fibers in pigs traverse the ventricular wall and extend nearly to the epicardial surface,(Tranum-Jensen et al., 1991) which make any lengthening of the QRS more relevant to other patho-physiological conditions with slower myocardial impulse propagation (e.g. right ventricular pacing). However, this *in-vivo* pig model undergoing increased left ventricular afterload does not resembles many of the structural and functional changes at different HF stages,(Jessup and Brozena, 2003) although it underscores that acute changes in ventricular wall stress are directly reflected on significant lengthening of the QRS complex. In fact, failing hearts with dilated cardiomyopathy (volume overload) and acute hemodynamic worsening with pressure overload should be theoretically more sensitive to widen the QRS complex.(Vest and Heupler Jr, 2013)

Interestingly, clinical series by Aranda *et al.* have shown that ~70% of patients with HF and normal sinus rhythm had their greatest QRS complex duration while hospitalized for decompensated HF.(Aranda et al., 2002) Moreover, regardless of mean QRS duration, patients with HF have significantly larger variability in time of QRS duration than patients without HF,(Aranda et al., 2002) which may reflect that HF patients are more exposed to hemodynamic, metabolic and pharmacological changes.

A challenging issue is to accurately measure QRS duration changes in patients with HF.(Madias, 2009) Moreover, QRS widening may not necessarily be related to an underlying decrease in CV as reported in a rabbit model of HF leading to myocardial hypertrophy after pressure and volume overload.(Wiegerinck et al., 2006) QRS duration may also be affected by other confounding factors commonly present in patients with HF,(Lancellotti et al., 2004) which increases the risk of false positive lengthening of the QRS; not associated with decompensated HF and pressure overload. Despite limitations to infer the exact underlying mechanism leading to QRS widening, current remote monitoring technology in patients with HF and ICD or CRT-D devices may enable to implement the following essential aspects to properly assess QRS duration: *i)* continuous monitoring of QRS duration trends over weekly periods using a can-tip/configuration, which is closer to a surface ECG lead than a true bipolar configuration; and *ii)* automated and reliable algorithms to detect QRS onset and offset with sufficient sample rate acquisition. Both technical aspects overcome some of the limitations present in many clinical series that manually measured QRS duration or relied on scarce ECG traces during the follow up.(Aranda et al., 2002; Wang et al., 2008; Xiao et al., 1996) Despite current technical advances to measure and monitoring QRS complex duration, a single parameter may probably be not enough to accurately monitor and predict HF hospitalizations and/or arrhythmic events. A combination of QRS duration as a surrogate of underlying CV disturbances, with other electrical parameters like T-wave alternans as a surrogate of underlying spatial gradients of repolarization,(Filgueiras-Rama, 2017; Quintanilla et al., 2015) might increase sensitivity and specificity to predict HF hospitalizations and/or arrhythmic events. Therefore, electrical parameters, using current remote monitoring technology and cloud-based big-data tools,(Lillo-Castellano et al., 2016) have the potential to identify underlying electrophysiological alterations present under high IVP and/or HF-ER, which are associated with higher risk of ventricular arrhythmia.(Quintanilla et al., 2015)

4.1. Limitations

Changes in QRS duration during sinus rhythm upon increasing afterload in pigs are not directly translated to humans, in whom the Purkinje system is on the endocardial surface.(Forsgren et al., 1982) However, changes may be larger in humans, especially in patients with HF, if sensitivity to myocardial wall stretch is similar between humans and pigs. Increasing afterload does not reproduce HF stages, although supports the notion of slower underlying CV upon increased myocardial wall stress.

The location of the pacing electrode outside the field of view, although close to it, precluded our CV measurements from including the slow axis of propagation. Therefore, the fact that failing hearts qualitatively showed higher propagation

anisotropy than controls (Figure 3A) could have somehow led to underestimate the reduction in CV upon increasing IVP in HF-ER hearts.

Sample rate acquisition during *in-vivo* experiments (100 Hz) does not enable to detect small changes in QRS duration, although 1-ms interpolation between consecutive samples partially overcame such limitation, along with a large number of ECG samples per animal. A certain degree of caution is warranted in interpreting the correlation coefficients in Figures 6C,D owing to their not very high explained variance that might be partially explained by inter-heart variability. Langendorff-perfused isolated hearts are denervated, which precludes accurate extrapolation to *in-vivo* conditions.

5. Conclusions

High IVP and/or HF-ER significantly decrease CV, which correlates with QRS widening on the volume-conducted ECG during ventricular pacing. Increased myocardial wall stress also widens the QRS complex during sinus rhythm *in-vivo*

6. Acknowledgment

We thank Alba García-Escolano for her support to signal processing.

7. Funding

The CNIC is supported by the Ministry of Economy, Industry and Competitiveness (MEIC) and the Pro CNIC Foundation, and is a Severo Ochoa Center of Excellence (SEV-2015-0505). This study was supported by grants from Fondo Europeo de Desarrollo Regional (FEDER), Instituto de Salud Carlos III [RD06/0003/0009 (REDINSCOR), RD12/0042/0036 (RIC),] and Spanish Ministry of Economy and Competitiveness (MINECO) (SAF2016-80324-R).

References

Abraham, W.T., Adamson, P.B., Bourge, R.C., Aaron, M.F., Costanzo, M.R., Stevenson, L.W., Strickland, W., Neelagaru, S., Raval, N., Krueger, S., Weiner, S., Shavelle, D., Jeffries, B., Yadav, J.S. and Group, C.T.S., 2011. Wireless pulmonary artery haemodynamic monitoring in chronic heart failure: a randomised controlled trial, Lancet. 377, 658-66.

Abraham, W.T. and Hayes, D.L., 2003. Cardiac resynchronization therapy for heart failure, Circulation. 108, 2596-603.

Adamson, P.B., Gold, M.R., Bennett, T., Bourge, R.C., Stevenson, L.W., Trupp, R., Stromberg, K., Wilkoff, B.L., Costanzo, M.R., Luby, A., Aranda, J.M., Heywood, J.T., Baldwin, H.A., Aaron, M., Smith, A. and Zile, M., 2011. Continuous hemodynamic monitoring in patients with mild to moderate heart failure: results of The Reducing Decompensation Events Utilizing Intracardiac Pressures in Patients With Chronic Heart Failure (REDUCEhf) trial, Congest Heart Fail. 17, 248-54.

Aranda, J.M., Carlson, E.R., Pauly, D.F., Curtis, A.B., Conti, C.R., Ariet, M. and Hill, J.A., 2002. QRS duration variability in patients with heart failure, Am J Cardiol. 90, 335-7.

Bourge, R.C., Abraham, W.T., Adamson, P.B., Aaron, M.F., Aranda, J.M., Jr., Magalski, A., Zile, M.R., Smith, A.L., Smart, F.W., O'Shaughnessy, M.A., Jessup, M.L., Sparks, B., Naftel, D.L., Stevenson, L.W. and Group, C.-H.S., 2008. Randomized controlled trial of an implantable continuous hemodynamic monitor in patients with advanced heart failure: the COMPASS-HF study, J Am Coll Cardiol. 51, 1073-9.

Brack, K.E., Narang, R., Winter, J. and Ng, G.A., 2013. The mechanical uncoupler blebbistatin is associated with significant electrophysiological effects in the isolated rabbit heart, Exp Physiol. 98, 1009-27.

Costanzo, M.R., Stevenson, L.W., Adamson, P.B., Desai, A.S., Heywood, J.T., Bourge, R.C., Bauman, J. and Abraham, W.T., 2016. Interventions Linked to Decreased Heart Failure Hospitalizations During Ambulatory Pulmonary Artery Pressure Monitoring, JACC Heart Fail. 4, 333-44.

Eijsbouts, S.C., Houben, R.P., Blaauw, Y., Schotten, U. and Allessie, M.A., 2004. Synergistic action of atrial dilation and sodium channel blockade on conduction in rabbit atria, J Cardiovasc Electrophysiol. 15, 1453-61.

Filgueiras-Rama, D., 2017. Sympathetic Innervation and Cardiac Arrhythmias, in: Zipes, D.P., Jalife, J. and Stevenson, W.G. (Eds.), Cardiac Electrophysiology: From Cell to Bedside. Elsevier.

Forsgren, S., Eriksson, A., Kjorell, U. and Thornell, L.E., 1982. The conduction system in the human heart at midgestation--immunohistochemical demonstration of the intermediate filament protein skeletin, Histochemistry. 75, 43-52.

Fukuta, H. and Little, W.C., 2008. The cardiac cycle and the physiologic basis of left ventricular contraction, ejection, relaxation, and filling, Heart Fail Clin. 4, 1-11.

Jessup, M. and Brozena, S., 2003. Heart failure, N Engl J Med. 348, 2007-18.

Kamkin, A., Kiseleva, I., Wagner, K.D., Bohm, J., Theres, H., Gunther, J. and Scholz, H., 2003. Characterization of stretch-activated ion currents in isolated atrial myocytes from human hearts, Pflugers Arch. 446, 339-46.

Lancellotti, P., Kulbertus, H.E. and Pierard, L.A., 2004. Predictors of rapid QRS widening in patients with coronary artery disease and left ventricular dysfunction, Am J Cardiol. 93, 1410-2, A9.

Lillo-Castellano, J.M., Marina-Breysse, M., Gomez-Gallanti, A., Martinez-Ferrer, J.B., Alzueta, J., Perez-Alvarez, L., Alberola, A., Fernandez-Lozano, I., Rodriguez, A., Porro, R., Anguera, I., Fontenla, A., Gonzalez-Ferrer, J.J., Canadas-Godoy, V., Perez-Castellano, N., Garofalo, D., Salvador-Montanes, O., Calvo, C.J., Quintanilla, J.G., Peinado, R., Mora-Jimenez, I., Perez-Villacastin, J., Rojo-Alvarez, J.L. and Filgueiras-Rama, D., 2016. Safety threshold of R-wave amplitudes in patients with implantable cardioverter defibrillator, Heart. 102, 1662-70.

Madias, J.E., 2009. QRS duration: problems in its implementation in patients with heart failure, Pacing Clin Electrophysiol. 32, 918-21.

Magalski, A., Adamson, P., Gadler, F., Boehm, M., Steinhaus, D., Reynolds, D., Vlach, K., Linde, C., Cremers, B., Sparks, B. and Bennett, T., 2002. Continuous ambulatory right heart pressure measurements with an implantable hemodynamic monitor: a multicenter, 12-month follow-up study of patients with chronic heart failure, J Card Fail. 8, 63-70.

Nattel, S., Maguy, A., Le Bouter, S. and Yeh, Y.H., 2007. Arrhythmogenic ion-channel remodeling in the heart: heart failure, myocardial infarction, and atrial fibrillation, Physiol Rev. 87, 425-56.

Ohlsson, A., Bennett, T., Nordlander, R., Ryden, J., Astrom, H. and Ryden, L., 1995. Monitoring of pulmonary arterial diastolic pressure through a right ventricular pressure transducer, J Card Fail. 1, 161-8.

Quintanilla, J.G., Moreno, J., Archondo, T., Usandizaga, E., Molina-Morua, R., Rodriguez-Bobada, C., Gonzalez, P., Garcia-Torrent, M.J., Filgueiras-Rama, D., Perez-Castellano, N., Macaya, C. and Perez-Villacastin, J., 2015. Increased intraventricular pressures are as harmful as the electrophysiological substrate of heart failure in favoring sustained reentry in the swine heart, Heart rhythm. 12, 2172-83.

Reiter, M.J., Stromberg, K.D., Whitman, T.A., Adamson, P.B., Benditt, D.G. and Gold, M.R., 2013. Influence of intracardiac pressure on spontaneous ventricular arrhythmias in patients with systolic heart failure: insights from the REDUCEhf trial, Circ Arrhythm Electrophysiol. 6, 272-8.

Stevenson, L.W., Zile, M., Bennett, T.D., Kueffer, F.J., Jessup, M.L., Adamson, P., Abraham, W.T., Manda, V. and Bourge, R.C., 2010. Chronic ambulatory intracardiac pressures and future heart failure events, Circ Heart Fail. 3, 580-7.

Tranum-Jensen, J., Wilde, A.A., Vermeulen, J.T. and Janse, M.J., 1991. Morphology of electrophysiologically identified junctions between Purkinje fibers and ventricular muscle in rabbit and pig hearts, Circ Res. 69, 429-37.

Vest, A.R. and Heupler Jr, F., 2013. Afterload, in: Anwaruddin, S., Martin, J.M., Stephens, J.C. and Askari, A.T. (Eds.), Cardiovascular Hemodynamics. Humana Press, pp. 29-51.

Wang, N.C., Maggioni, A.P., Konstam, M.A., Zannad, F., Krasa, H.B., Burnett, J.C., Jr., Grinfeld, L., Swedberg, K., Udelson, J.E., Cook, T., Traver, B., Zimmer, C., Orlandi, C., Gheorghiade, M. and Efficacy of Vasopressin Antagonism in Heart Failure Outcome Study With Tolvaptan, I., 2008. Clinical implications of QRS duration in patients hospitalized with worsening heart failure and reduced left ventricular ejection fraction, JAMA. 299, 2656-66.

Wiegerinck, R.F., Verkerk, A.O., Belterman, C.N., van Veen, T.A., Baartscheer, A., Opthof, T., Wilders, R., de Bakker, J.M. and Coronel, R., 2006. Larger cell size in rabbits with heart failure increases myocardial conduction velocity and QRS duration, Circulation. 113, 806-13.

Xiao, H.B., Roy, C., Fujimoto, S. and Gibson, D.G., 1996. Natural history of abnormal conduction and its relation to prognosis in patients with dilated cardiomyopathy, Int J Cardiol. 53, 163-70.

Zile, M.R., Adamson, P.B., Cho, Y.K., Bennett, T.D., Bourge, R.C., Aaron, M.F., Aranda, J.M., Jr., Abraham, W.T., Stevenson, L.W. and Kueffer, F.J., 2011. Hemodynamic factors associated with acute decompensated heart failure: part 1--insights into pathophysiology, J Card Fail. 17, 282-91.

Zile, M.R., Bennett, T.D., El Hajj, S., Kueffer, F.J., Baicu, C.F., Abraham, W.T., Bourge, R.C. and Warner Stevenson, L., 2017. Intracardiac Pressures Measured Using an Implantable Hemodynamic Monitor: Relationship to Mortality in Patients With Chronic Heart Failure, Circ Heart Fail. 10.

Zile, M.R., Bennett, T.D., St John Sutton, M., Cho, Y.K., Adamson, P.B., Aaron, M.F., Aranda, J.M., Jr., Abraham, W.T., Smart, F.W., Stevenson, L.W., Kueffer, F.J. and Bourge, R.C., 2008. Transition from chronic compensated to acute decompensated heart failure: pathophysiological insights obtained from continuous monitoring of intracardiac pressures, Circulation. 118, 1433-41.

Figures legends

Figure 1. Experimental setting in isolated hearts and processing of optical signals. A: Schematic representation of a Langendorff-perfused pig heart preparation, volume-conducted ECG and optical mapping. ECG electrodes submerged in the superfusion Tyrode´s are depicted in blue. Of note, ECG electrodes are not placed at specific stationary locations during the experiment. **B:** Activation and velocity map from optical recordings (upper panel). Example of activation times at the time of $(dV/dt)_{max}$ at 4 locations (1-4) on the field of view (bottom panel). The blue tracings display the preconditioned optical action potentials. The green tracings display these optical action potentials after low-pass Butterworth filtering. The first derivative is performed over these filtered potentials (black tracings), showing a clear and unique absolute maximum at the time of activation.

Figure 2. Experimental setting and data acquisition in pigs undergoing high left ventricular afterload. A: Open chest view of the ascending aorta. The surgical strips around the aorta indicate the region to perform partial clamping of the aorta. **B:** X-Ray view of the proximal *(pigtail catheter 1)* and distal *(pigtail catheter 2)* pigtail catheters**. C:** Example of automatic QRS onset and offset determination in a surface ECG signal (lead V1) obtained from one pig. The black tracing displays the surface ECG signal after 10x interpolation between samples. The first derivative is performed over this signal and then rectified (red tracing, absolute value of ECG slope) and smoothed (purple tracing) with local regression using weighted linear least squares and a 2^{nd} degree polynomial model. The times when the purple tracing crosses a 4% threshold of the maximum slope value are detected as QRS onset and offset. These times are displayed as dark blue dotted lines.

Figure 3. *Ex-vivo* CV measurements in control and failing hearts under low and high IVP, during S1 and S2 paced wavefronts. CV data were suitable for analysis in 7 control and 6 HF hearts. **A:** sample activation maps and CV vectors in a control and a failing heart at 300 ms BDCL. The average of the CV magnitudes is displayed. The size of the displayed vectors is automatically adjusted in order to prevent vectors from overlapping. Therefore, their sizes are not comparable among different maps from different wavefronts. **B:** Depicted data at 500 ms BDCL, and **B:** depicted data at 300 ms BDCL**.** The p values displayed here are global (results from tests of model effects). **C:** Relative change in paired measurements of CV (%).BDCL: basic drive cycle length; Extra: extrastimuli. HF-ER: heart failure electrophysiological remodeling; IVP: intraventricular pressure.

Figure 4. *Ex-vivo* volume-conducted QRS measurements in control and failing hearts under low and high IVP, in S1 and S2 paced wavefronts. QRS complex duration was suitable for analysis in 7 control and 5 HF hearts. **A:** Depicted data at 500 ms BDCL (left panel) and at 300 ms BDCL (right panel). **B:** HF-ER*IVP interaction. **C:** Relative change in paired measurements of QRS duration (%). The p values displayed here are global (results from tests of model effects). Abbreviations as in Figure 3.

Figure 5. Sample QRS complex prolongation in *ex-vivo* Langendorff-perfused hearts at 500 ms BDCL under low (leftmost panel) and high (rightmost panel) IVP. **Top:** Control heart. **Bottom:** Failing heart. Four volume-conducted ECG leads

are shown on each panel. Vertical blue lines show the QRS onset and QRS offset during S1 and S2 pacing. Up to 4 leads may be required to appropriately detect the QRS onset and offset. QRS is longer in the failing heart than in the control heart. High IVP increased S1 and S2-related QRS complex duration as a result of decreased conduction velocity in the ventricular tissue of both control and failing hearts upon increasing IVP. Abbreviations as in Figure 3.

Figure 6. **Correlation between QRS complex duration and left ventricular afterload.** The data displayed were obtained from 3 pigs. **A,B:** Aortic root pressure increases and descending aorta (DA) pressure decreases upon partially clamping the ascending aorta. **C,D:** QRS complex duration broadens during sinus rhythm after increasing LV afterload *in-vivo.*

Figure 7. Sample QRS complex duration in a pig undergoing high left ventricular afterload**.** QRS complex during sinus rhythm widened from 80 ms at baseline (top left panel) to 100 ms under high left ventricular afterload (top right panel). Aortic pressures in the proximal (aortic root) and distal aorta (descending aorta) are depicted on the bottom. Y-axis labeling has been adjusted from low to high left ventricular afterload.

Figure 1

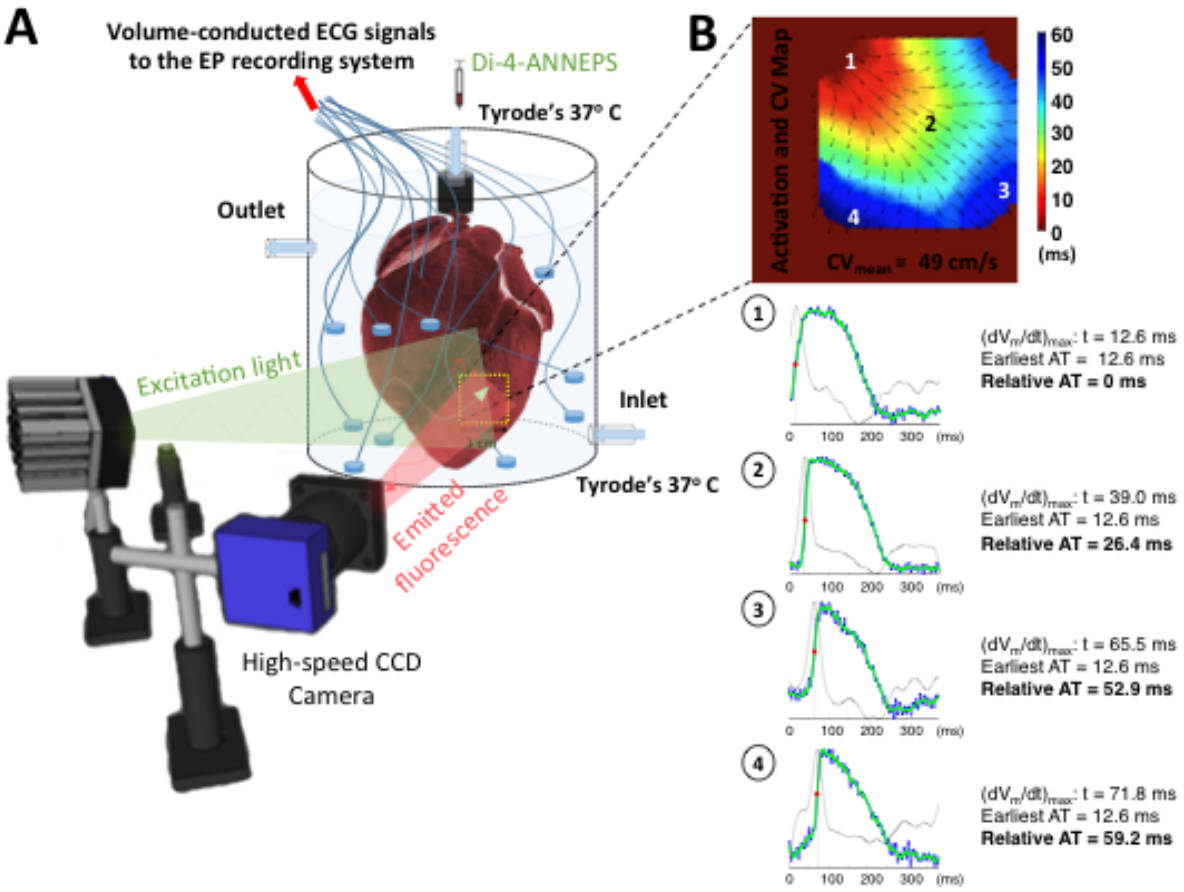
A
Volume-conducted ECG signals
to the EP recording system
Di-4-ANNEPS
Tyrode's 37° C
Outlet
Excitation light
Inlet
Tyrode's 37° C
Emitted
fluorescence
High-speed CCD
Camera
B
Activation and CV Map
1
2
3
4
CV mean = 49 cm/s
60
50
40
30
20
10
0
(ms)
(dVm/dt)max: t = 12.6 ms
Earliest AT = 12.6 ms
Relative AT = 0 ms
(dVm/dt)max: t = 39.0 ms
Earliest AT = 12.6 ms
Relative AT = 26.4 ms
(dVm/dt)max: t = 65.5 ms
Earliest AT = 12.6 ms
Relative AT = 52.9 ms
(dVm/dt)max: t = 71.8 ms
Earliest AT = 12.6 ms
Relative AT = 59.2 ms
0 100 200 300 (ms)

Figure 2

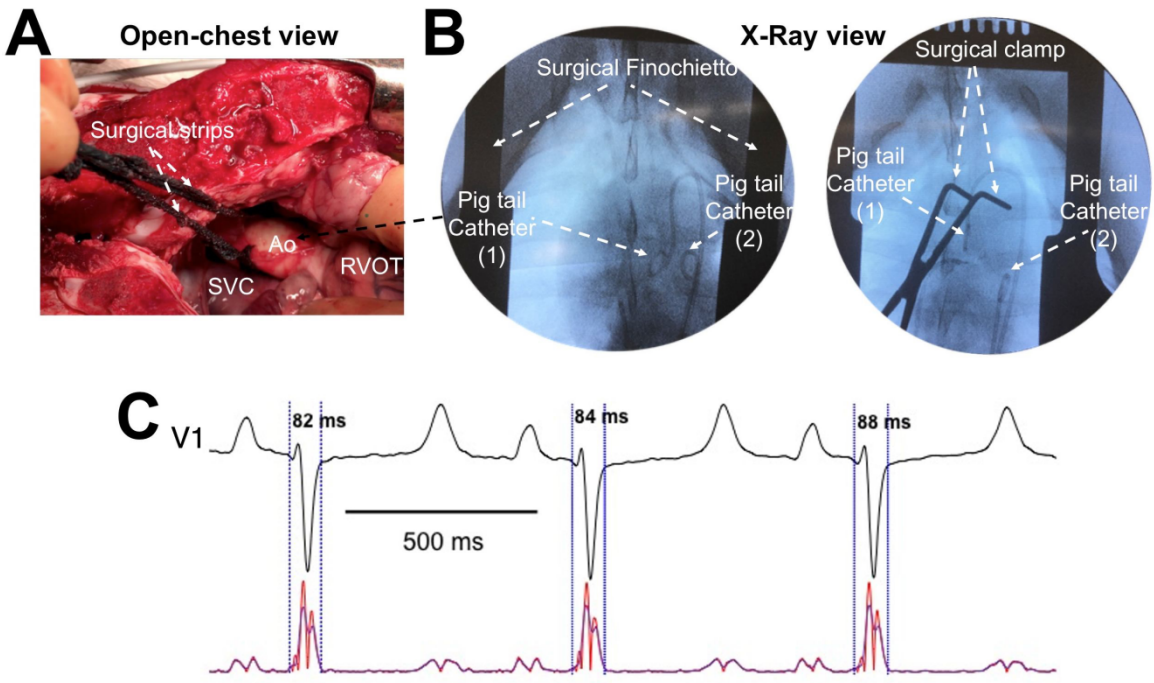
A
Open-chest view
Surgical strips
Ao
RVOT
SVC
B
X-Ray view
Surgical Finochietto
Pig tail Catheter (1)
Pig tail Catheter (2)
Surgical clamp
Pig tail Catheter (1)
Pig tail Catheter (2)
C
V1
82 ms
84 ms
88 ms
500 ms

Figure 3

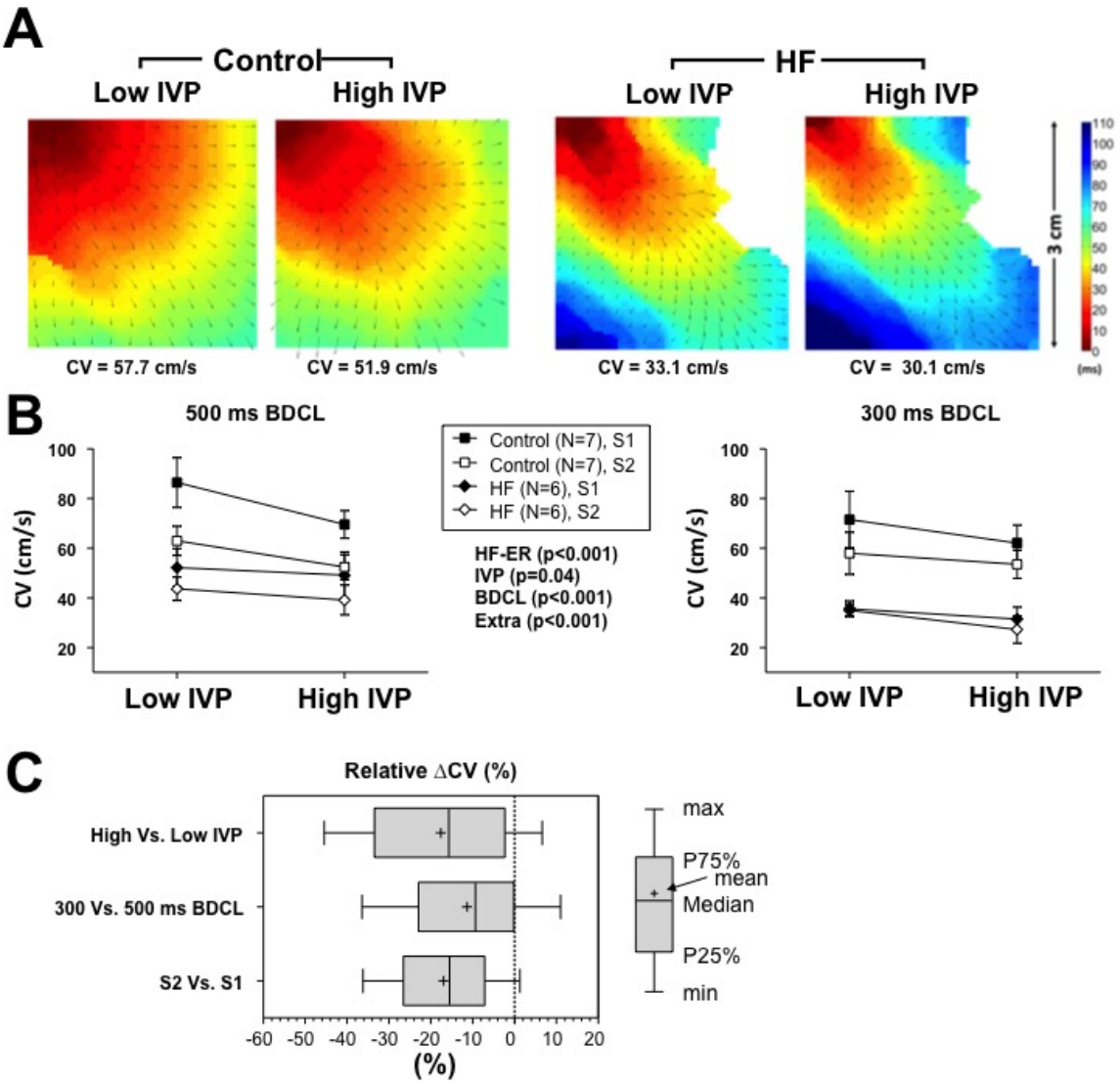
A
Control
HF
Low IVP
High IVP
Low IVP
High IVP
CV = 57.7 cm/s
CV = 51.9 cm/s
CV = 33.1 cm/s
CV = 30.1 cm/s
3 cm
(ms)
B
500 ms BDCL
300 ms BDCL
CV (cm/s)
Control (N=7), S1
Control (N=7), S2
HF (N=6), S1
HF (N=6), S2
HF-ER (p<0.001)
IVP (p=0.04)
BDCL (p<0.001)
Extra (p<0.001)
Low IVP
High IVP
C
Relative ΔCV (%)
High Vs. Low IVP
300 Vs. 500 ms BDCL
S2 Vs. S1
(%)
max
P75%
mean
Median
P25%
min

Figure 4

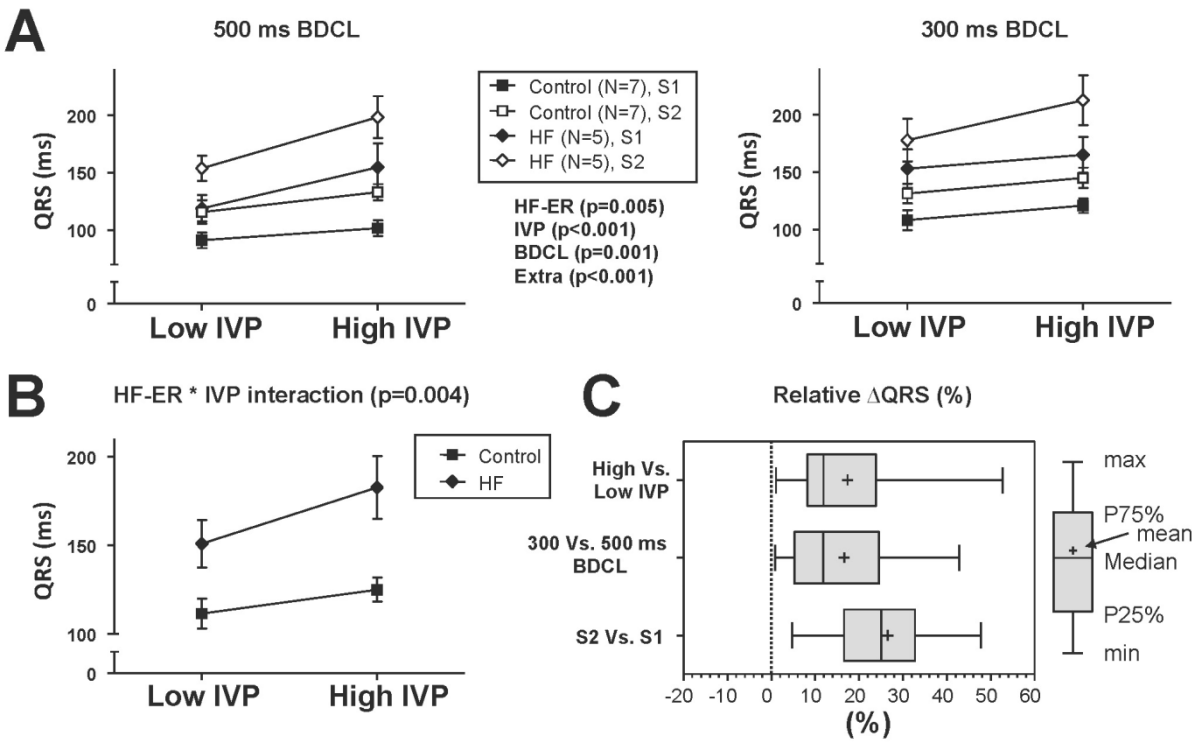
A
500 ms BDCL
300 ms BDCL
QRS (ms)
200
150
100
0
Low IVP
High IVP
Control (N=7), S1
Control (N=7), S2
HF (N=5), S1
HF (N=5), S2
HF-ER (p=0.005)
IVP (p<0.001)
BDCL (p=0.001)
Extra (p<0.001)
B
HF-ER * IVP interaction (p=0.004)
Control
HF
C
Relative ΔQRS (%)
High Vs. Low IVP
300 Vs. 500 ms BDCL
S2 Vs. S1
-20 -10 0 10 20 30 40 50 60
(%)
max
P75%
mean
Median
P25%
min

Figure 5

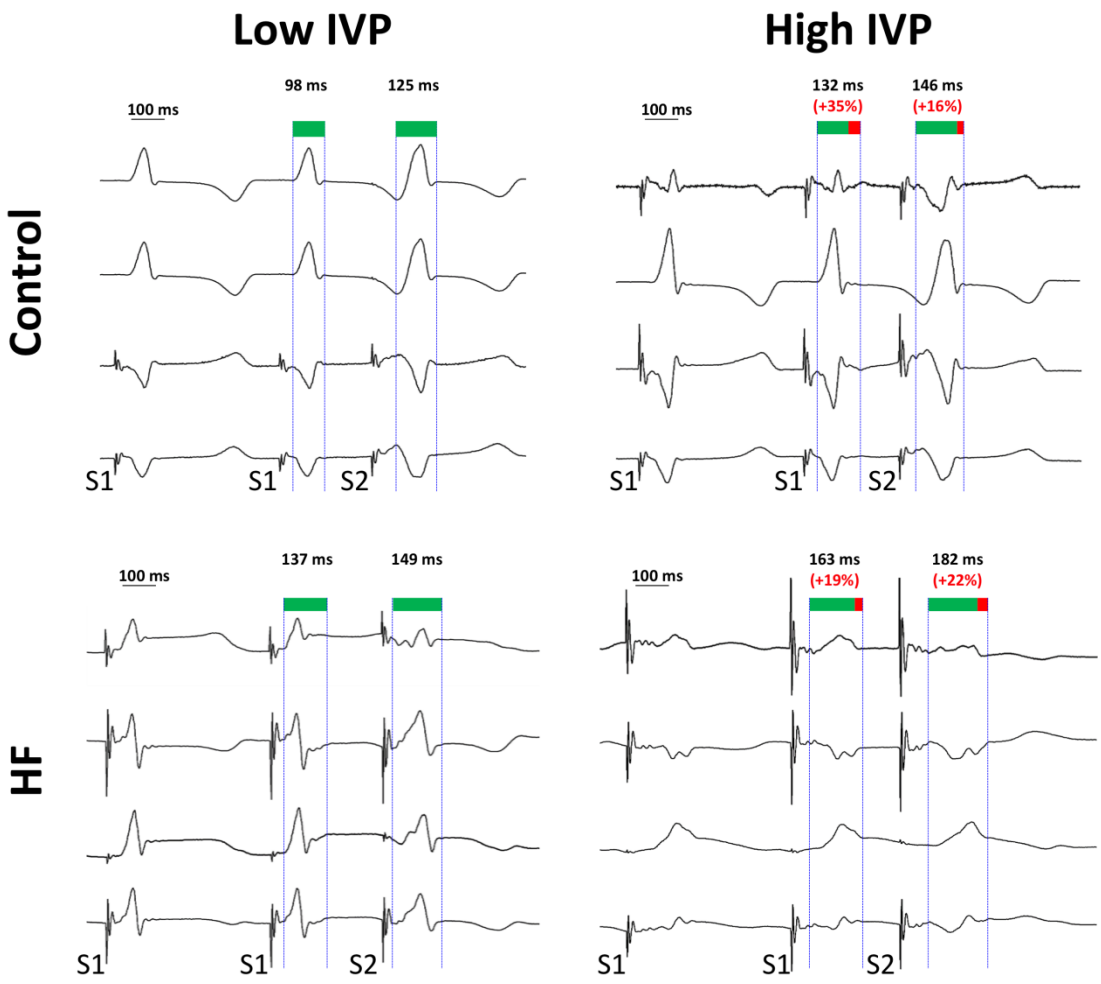
Low IVP
High IVP
Control
HF
100 ms
98 ms
125 ms
132 ms
(+35%)
146 ms
(+16%)
137 ms
149 ms
163 ms
(+19%)
182 ms
(+22%)
S1
S1
S2

Figure 6

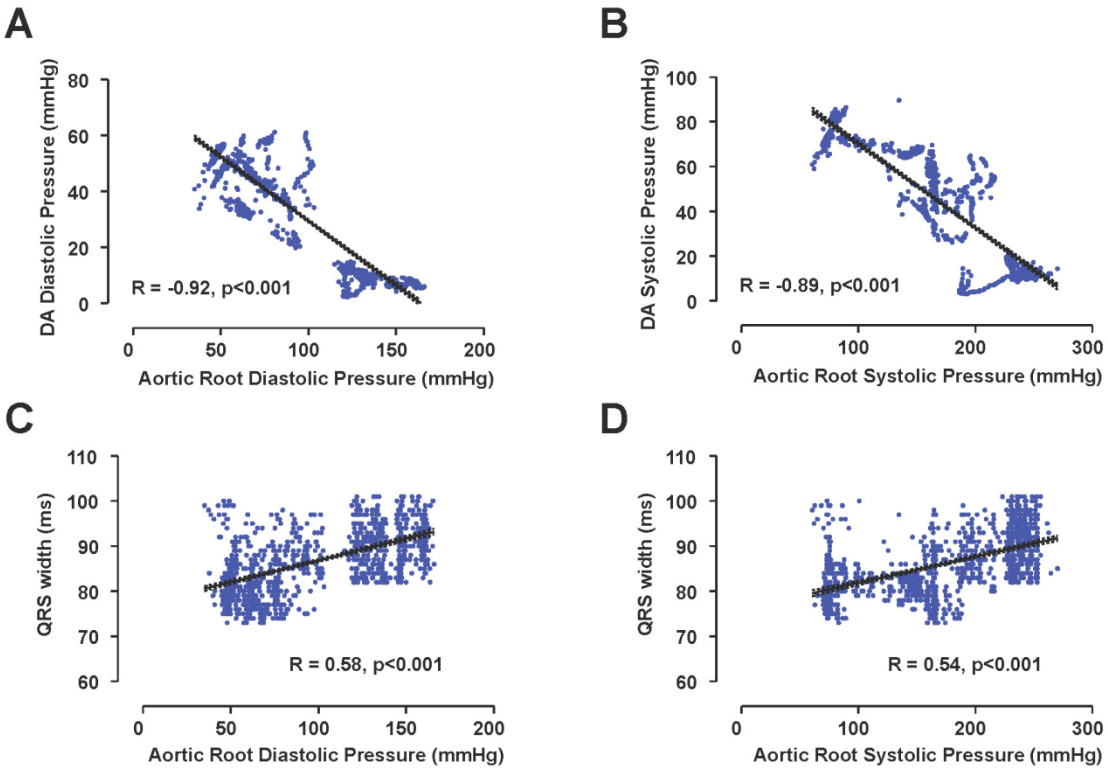
A
DA Diastolic Pressure (mmHg)
80
60
40
20
0
R = -0.92, p<0.001
0
50
100
150
200
Aortic Root Diastolic Pressure (mmHg)
B
DA Systolic Pressure (mmHg)
100
80
60
40
20
0
R = -0.89, p<0.001
0
100
200
300
Aortic Root Systolic Pressure (mmHg)
C
QRS width (ms)
110
100
90
80
70
60
R = 0.58, p<0.001
0
50
100
150
200
Aortic Root Diastolic Pressure (mmHg)
D
QRS width (ms)
110
100
90
80
70
60
R = 0.54, p<0.001
0
100
200
300
Aortic Root Systolic Pressure (mmHg)

Figure 7

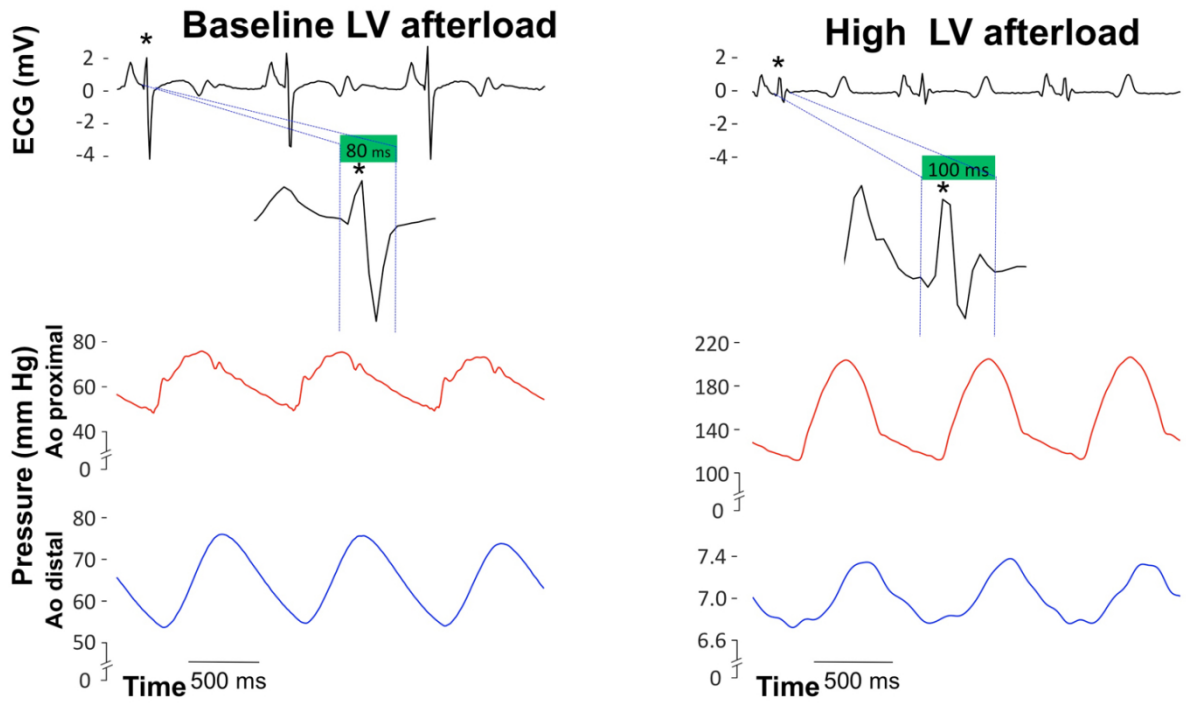
Baseline LV afterload
High LV afterload
ECG (mV)
2
0
-2
-4
80 ms
100 ms
Pressure (mm Hg)
Ao proximal
80
60
40
0
Ao distal
80
70
60
50
0
220
180
140
100
0
7.4
7.0
6.6
0
Time
500 ms

Tables

Table 1

QRS duration(ms)				
			Low IVP	**High IVP**
Control	**500 ms**	**S1**	91.1 ± 6.9	101.6 ± 6.7
		S2	115.7 ± 10.3	133.0 ± 7.09
	300 ms	**S1**	108.1 ± 8.8	120.7 ± 6.2
		S2	131.3 ± 8.6	145.0 ± 8.9
HF	**500 ms**	**S1**	119.0 ± 11.5	154.6 ± 21.1
		S2	153.8 ± 11.1	198.4 ± 18.2
	300 ms	**S1**	153.0 ± 16.7	165.0 ± 15.7
		S2	177.8 ± 18.5	212.6 ± 21.7
	Test of Model Effects (GEE)			**P-value**
2-way interactions	HF*IVP			**0.004**
	HF*BDCL			0.665
	HF*Extra			0.071
	IVP*BDCL			0.077
	IVP*Extra			**<0.001**
	BDCL*Extra			0.299

BDCL: Basic Drive Cycle Length; Extra: Extrastimuli;
GEE: Generalized Estimating Equations;
HF: Heart Failure; IVP: Intraventricular Pressure;